Green Relay Assisted D2D Communications with Dual Batteries in Heterogeneous Cellular Networks for IoT

Green Relay Assisted D2D Communications with Dual Batteries in Heterogeneous Cellular Networks for IoT

Xilong Liu, *Student Member, IEEE* and Nirwan Ansari, *Fellow, IEEE*

***Abstract*—The Internet of Things (IoT) heralds a vision of future Internet where all physical things/devices are connected via a network to promote a heightened level of awareness about our world and dramatically improve our daily lives. Nonetheless, most wireless technologies in unlicensed band cannot provision ubiquitous and quality IoT services. In contrast, cellular networks support large-scale, quality of service guaranteed and secured communications. However, tremendous proximal communications via local base stations (BSs) will lead to severe traffic congestion and huge energy consumption in conventional cellular networks. Device-to-Device (D2D) communications can potentially offload traffic from and reduce energy consumption of BSs. In order to realize the vision of a truly global IoT, we propose a novel architecture, i.e., overlay based green relay assisted D2D communications with dual batteries in heterogeneous cellular networks. By optimally allocating the network resource, our proposed resource allocation method provisions the IoT services and minimizes the overall energy consumption of the pico relay BSs. By balancing the residual green energy among the pico relay BSs, the green energy utilization has been maximized; this furthest saves the on-grid energy. Finally, we validate the performance of the proposed architecture through extensive simulations.**

***Index Terms*—IoT, D2D communications, dual batteries, resource allocation, heterogeneous networks.**

I. Introduction

THE Internet of Things (IoT) heralds a vision of future Internet where all the physical things are connected through a network to exchange information about themselves and their surroundings. IoT promotes a heightened level of awareness about our world and bestows intelligence in our daily lives. Physical things are embedded with electronics, software, sensing ability and network connectivity, and are thus enabled to gather, share, forward information and collaborate with each other. Examples of such things can be sensors, health care gadgets, mobile phones, smart meters, home appliances, and even smart furnitures and vehicles. In general, all these featured things are referred to as devices. IoT can enrich our lives and improve our daily experience by providing a platform for connecting all the possible devices cooperatively [1].

A large number of IoT applications are emerging. For example, in the residential area, smart homes can be facilitated by IoT via home appliance automation control. In hospitals, various medical facilities can sense and cooperate to provide prompt patient services. In factories and farms, instruments can collaborate with each other to enhance the performance and efficiency of factory and farm operations. IoT also enables vehicle-to-vehicle and vehicle-to-person communications to improve traffic management and transportation safety. There are many other IoT application scenarios, such as context aware smart space, proximal files sharing, proximal social networking and fog computing.

Wireless solutions to realizing IoT are critical owing to pervasiveness of emerging mobile IoT devices. However, most wireless technologies which work in unlicensed bands cannot provision the ubiquitous, seamless and quality service required for IoT. For instance, Zigbee only enables low data rate transmission, and single channel incurs dense interference; Bluetooth is limited to short range transmission and is sensitive to fading and interference; Low Power Wide Area (LPWA) only allows low data rate transmission and is sensitive to fading as well, and lacks scalability for large-scale IoT [2]; WiFi suffers from poor mobility and roaming support, and does not offer guaranteed quality of services (QoS), due to high interference caused by sharing the unlicensed 2.4 GHz band with Zigbee, Bluetooth, and many other unlicensed band technologies [3]. As compared to unlicensed band technologies, cellular networks provide global coverage, resource management and QoS guaranteed and secured services as well as mobility and roaming support.

Stimulated by the emerging IoT market, the cellular providers are introducing IoT functionalities into their networks [4], [5]. However, a large number of proximal devices communicating through a local base station (BS) in a conventional cellular network will incur severe traffic congestion, high latency, and huge energy consumption at BS. Therefore, Device-to-Device (D2D) communications has received much attention in cellular networks [4], in which the source and destination devices can directly communicate with minimal assistance from BS, thus providing multiple performance benefits. First, due to the short range communications, proximal D2D devices can enjoy high data rates with low end-to-end delay and low energy consumption. Second, it is more resource-efficient for proximal devices to communicate directly than routing through an involved BS and possibly core network [5]. Third, direct path offloads cellular traffic in BSs and network,

X. Liu and N. Ansari are with Advanced Networking Laboratory, Helen & John C. Hartmann Department of Electrical and Computer Engineering, New Jersey Institute of Technology, Newark, NJ 07102 USA (email: xl249@njit.edu; nirwan.ansari@njit.edu). This work was supported in part by NSF under grant no. CNS-1320468.

thus alleviating congestion, and consequently benefiting other non-D2D users as well [5].

In order to improve spectrum efficiency, existing D2D communications leverages the underlay spectrum sharing approach in homogeneous cellular network. In this approach, D2D transmissions reuse the spectrum of the cellular network, and are thus subject to the interference caused by the cellular users; inversely, the cellular communications can also be interfered by D2D users. Many works have been proposed to alleviate this interference issue. However, most of their bandwidth allocation and power control problems are NP-hard. Although some heuristics have been proposed to reduce the runtime, the interference still cannot be eliminated [6]. These works are only tenable with dozens of active D2D devices in a macrocell. When the number of D2D devices increases to realize the large-scale and ubiquitous IoT, the mutual interference is insurmountable. In addition, in their underlay schemes, cellular users are served with high priority [7], while D2D services are not guaranteed.

It is imperative to decouple D2D communications from the occupied cellular spectrum to facilitate ubiquitous, seamless and quality services required for IoT. By leveraging the overlay spectrum sharing approach, D2D and cellular communications are to be accommodated on separated spectra to avoid the mutual interference. This is beneficial to both cellular and D2D users. There is a constant demand for new spectral bands to boost the new generation of communications [8], [9]. In fact, on July 14, 2016, FCC voted to open up almost 11 GHz of spectrum for wireless communications [10]. Besides utilizing licensed spectrum, portions of unlicensed spectrum have been proposed to be integrated into Long-Term Evolution (LTE) cellular networks to facilitate IoT and D2D communications [11], [12]. Therefore, we assume additional spectrum will be dedicated for D2D communications in realizing IoT.

Powering BSs with green energy can effectively reduce on-grid energy consumption and carbon footprints. Since both green energy generation and communication workloads at individual BSs exhibit temporal and spatial diversities, the mismatch between the available green energy and workload demanded energy at BSs leads to poor utilization of green energy [13]. Therefore, to furthest save the on-grid energy, maximizing the utilization of green energy has become a common goal [14], [15]. Most existing works propose green energy related algorithms by assuming the generation rate of green energy can be perfectly predicted. However, it is difficult to know the accurate green energy generation rate in advance because it depends on many factors. Even though some estimation models have been proposed, they are grossly inaccurate for green energy prediction [16]. Hence, we propose a dual batteries system to harvest, store and utilize green energy. By installing dual batteries at BSs, the amount of available green energy in each time period is known and accurate.

By taking into account of all these issues comprehensively, in order to actualize the vision of a truly global IoT, we propose a novel architecture, i.e., overlay based green relay assisted Device-to-Device communications with dual batteries in heterogeneous cellular networks for IoT,[1] as shown in Fig. 1. By leveraging existing cellular infrastructure, we adopt the low power pico BSs as the relay BSs to facilitate D2D communications. IoT devices are assumed to be driven by the unified D2D communications protocol. By optimally allocating the network resource, our proposed resource allocation method fulfills the required IoT service data rates and minimizes the overall energy consumption of the relay BSs. To supplement energy provisioning, the relay BSs are equipped with solar panels and dual batteries to harvest and utilize green energy. Also, the relay BSs are connected by networking cables/fibers and electric transmission lines, for sharing the D2D routing information and maximizing the green energy utilization, respectively.

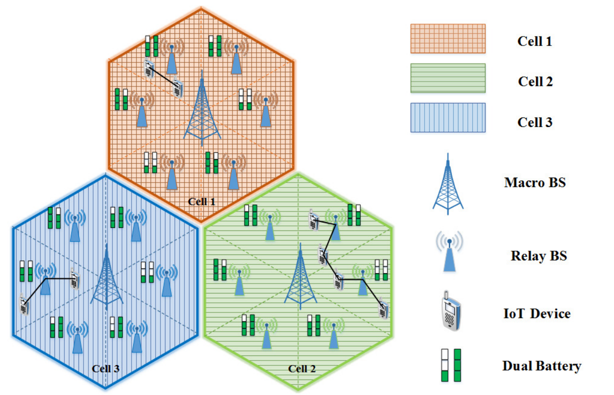

Fig. 1. The architecture of green relay assisted D2D communication with dual batteries system in a heterogeneous cellular network.

II. System Model

Consider a heterogeneous cellular network with multiple macro BSs and pico BSs (pico BSs act as relay BSs) as shown in Fig. 1. The macro BSs are evenly placed according to a hexagonal grid. Spectrum reuse factor is the rate at which the same frequency can be used in the network. In this work, the spectrum reuse factor for cellular frequency planning is $1/3$, which means 3 adjacent macrocells, for example, Cells 1, 2 and 3, cannot utilize the same spectral band. Thus, two adjacent macrocells will have no interference [17], [18]. We adopt the overlay spectrum sharing approach to facilitate D2D communications, and there is no interference between D2D and cellular network. All the macro BSs and relay BSs in this network are synchronized and coordinated. Assume the relay BSs within a macrocell can cooperatively cover this macrocell completely, and so any device within this macrocell can be served by the relay BSs.

A. Direct D2D Communications Group

For each picocell, the channel state information (CSI) between the devices, and that between the devices and the relay BS are assumed known by the relay BS [17], [19]. CSI includes multiple channel state factors, such as path loss, shadowing and fading. According to CSI in every time slot, we partition the devices within a picocell into two groups. If

[1]The initial idea about overlay based green relay assisted D2D communications for IoT was first presented at IEEE Globecom 2016 [1].

the channel state in a source-destination (SD) device pair is better than the channel state between the source device and the relay BS, this SD pair is classified into the direct D2D group, in which the source device can directly transmit data to the destination device. As shown in Fig. 2, the solid line represents the direct D2D transmission.

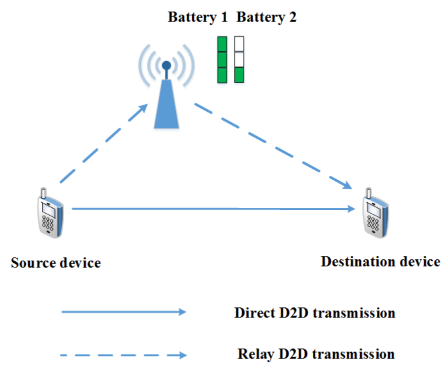

Fig. 2. Direct and relay D2D communications.

Let M be the number of SD pairs in the direct D2D group under the coverage of a particular relay BS j; denote $S_{Direct} = (s_1, s_2, ..., s_m)$ and $D_{Direct} = (d_1, d_2, ..., d_m)$ as the source and destination devices in this group, respectively. Single-carrier frequency division multiple access (SC-FDMA) is adopted in the transmission between devices [20]. So, there is no interference within a picocell. Different picocells carve up and utilize all the orthogonal channels of this macrocell [21]. Hence, there is no interference between the picocells within the same macrocell. As aforementioned, there is no inter-macrocell interference, and hence, the transmission data rate for the mth SD pair is

$$C^{SD}_{m,j} = W^S_{m,j} log_2(1 + \frac{P^S_{m,j} h^{SD}_{m,j}}{N_0 W^S_{m,j}}). \quad (1)$$

Here, $P^S_{m,j}$ is the transmission power of the mth source device in picocell j, $h^{SD}_{m,j}$ the channel gain between the mth source and destination device in picocell j, N_0 the power spectral density of additive white Gaussian noise (AWGN), and $W^S_{m,j}$ the bandwidth allocated to the mth SD pair in the jth picocell.

B. Relay Assisted Dual-hop D2D Communications Group

According to CSI, if the channel state between the source device and the relay BS is better than or equal to that in an SD pair, this SD pair is classified into the relay assisted dual-hop D2D group (for simplicity, relay D2D group), because the channel state favors the transmission from the source device to the relay BS. The relay BS can relay the information for the source device to its corresponding destination device with an equal or higher data rate. In this case, the source device saves energy by sending data to the relay BS, instead of being constrained from transmitting to the destination device in a poor quality link. As shown in Fig. 2, the dash line refers to the relay D2D transmission.

Let N be the number of SD pairs in the relay D2D group under the coverage of the relay BS j, and $S_{Relay} = (s'_1, s'_2, ..., s'_n)$ and $D_{Relay} = (d'_1, d'_2, ..., d'_n)$ denote the sets of source and destination devices, respectively. Similarly, without interference, the transmission data rate for the nth source device to relay BS (SR link) is

$$C^{SR}_{n,j} = W^S_{n,j} log_2(1 + \frac{P^S_{n,j} h^{SR}_{n,j}}{N_0 W^S_{n,j}}). \quad (2)$$

Here, $P^S_{n,j}$ is the transmission power of the nth source device in the jth picocell. $h^{SR}_{n,j}$ is the channel gain between the nth source device and the relay BS j. $W^S_{n,j}$ is the bandwidth allocated to the nth source device.

The transmission data rate for the relay BS for serving the nth destination device (RD link) is

$$C^{RD}_{n,j} = W^R_{n,j} log_2(1 + \frac{P^R_{n,j} h^{RD}_{n,j}}{N_0 W^R_{n,j}}). \quad (3)$$

Here, $P^R_{n,j}$ is the transmission power of the jth relay BS for serving the nth destination device. $h^{RD}_{n,j}$ is the channel gain between the relay BS j and nth destination device. $W^R_{n,j}$ is the bandwidth allocated for serving the nth destination device.

For the relay assisted dual-hop D2D communications, the nth source device sends the data to the relay BS in the first time unit, and then the relay BS sends the received data to the nth destination device in the second time unit [22], and hence the effective data rate of this SD pair is

$$C^{SD}_{n,j} = \frac{1}{2} \min \{C^{SR}_{n,j}, C^{RD}_{n,j}\}. \quad (4)$$

III. Network Resource Allocation Optimization

Our proposed architecture facilitates not only intra-picocell D2D communications, but also multi-hop inter-pico/macrocell D2D communications by sharing the routing information among pico/macro BSs. The source device will first inquire the IP/MAC addresses of the destination device at the local relay BS, and if the destination device is in the same picocell, the relay BS will establish the intra-picocell D2D transmission for this SD pair; otherwise, the local relay BS will schedule a routing path for this source device, i.e., the relay BS first relays the information to an intermediate device located at its coverage boundary, and then this intermediate device will be guided to associate with the neighboring relay BS in the next time slot, and forward the information to that neighboring relay BS or to other device guided by that neighboring relay BS. The information being delivered among different picocells or macrocells is eventually delivered to the destination device.

Within the coverage of a relay BS, no matter whether the transmission is a complete transmission of intra-picocell D2D communications or a partial transmission of multi-hop inter-pico/macrocell transmission, there always involves one SD pair under the coverage of a relay BS. Therefore, we perform the resource allocation optimization for the two groups of SD pairs within the relay BSs of each macrocell in each time slot.

A. Resource Allocation for the Direct D2D Group

Consider J picocells in one macrocell. $P^S_{m,j}$ is the transmission power of the mth source device in the direct D2D group in the jth picocell. Different types of devices have different transmission power $P^S_{m,j}$, and for the same source device its $P^S_{m,j}$ can also be different in different time slots. In this work, we assume in each time slot, $P^S_{m,j}$ of each device is fixed and known by the relay BS through the control link before the transmission [23]. Denote $C^{SD}_{m\_req,j}$ as the required data rate of the IoT application of the mth SD pair; $C^{SD}_{m\_req,j}$ can be different in different time slots for different SD pairs; assume they are fixed and known by the relay BS for each time slot. The channel gain $h^{SD}_{m,j}$ and noise power spectral density N_0 in Eq. (1) remain constant within each time slot. The resource allocation scheme for the devices in the direct D2D group is to assign the proper bandwidth for each SD pair's data rate $C^{SD}_{m,j}$ to reach its required service data rate $C^{SD}_{m\_req,j}$, i.e.,

$$C^{SD}_{m,j} = C^{SD}_{m\_req,j} = W^S_{m,j} log_2(1 + \frac{P^S_{m,j} h^{SD}_{m,j}}{N_0 W^S_{m,j}}). \quad (5)$$

Here, $W^S_{m,j}$ is the only variable in Eq. (5). According to Shannon's Theorem [24], for a fixed $P^S_{m,j}$, by increasing its transmission bandwidth $W^S_{m,j}$, the data rate will be increased accordingly. Also, note that $C^{SD}_{m,j}$ is a concave increasing function of $W^S_{m,j}$ for a fixed $P^S_{m,j}$ [25]; by increasing $W^S_{m,j}$, the transmission data rate $C^{SD}_{m,j}$ will be increased. Therefore, properly allocating bandwidth to each SD pair in the direct D2D group can facilitate the data rate to satisfy their application required service data rate. The occupied bandwidth for the direct D2D group in the jth picocell is $W_{Direct,j} = \sum_{m=1}^{M} W^S_{m,j}$. Thus, the occupied bandwidth for the direct D2D group in this macrocell is $W_{Direct} = \sum_{j=1}^{J} W_{Direct,j}$.

B. Resource Allocation for the Relay D2D Group

Suppose the total available spectrum bandwidth for IoT D2D communications in a macrocell is W_{D2D}. We have obtained the occupied bandwidth for the direct D2D group in this macrocell as W_{Direct}, and so the remaining bandwidth for the relay D2D group is $W_{Relay} = W_{D2D} - W_{Direct}$. The transmission of the relay D2D group concurs with that of the direct D2D group within the same time slot. In order to schedule the transmission and optimize the resource allocation for the relay D2D group, the time slot for the relay D2D transmission is further evenly divided into two sub-time slots, as shown in Fig. 3. The first sub-time slot is for the source device to the relay BS (SR link) transmission; the second sub-time slot is for the relay BS to the destination device (RD link) transmission. The available bandwidth for the relay D2D group W_{Relay} is fully used in the first sub-time slot, and then fully used in the second sub-time slot again.

1) First Sub-time Slot Resource Allocation Optimization: Again, consider J picocells in a macrocell. For all the devices in the relay D2D groups of these J picocells, in the first sub-time slot, each relay BS will allocate the bandwidth to each source device within its own picocell coverage. The optimization objective is to maximize the overall data rates from all the source devices to their corresponding relay BSs, i.e., maximizing the overall data rates at the SR links for all these J picocells, while guaranteeing half of the data rate

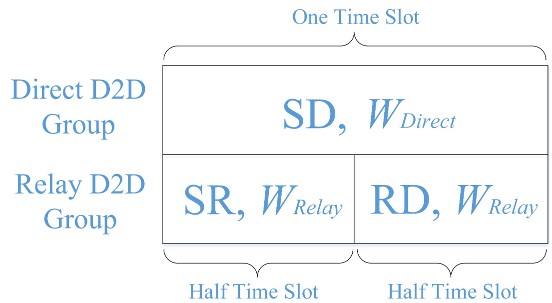

Fig. 3. Resource allocation framework within one time slot.

of each SR link $\frac{1}{2}C^{SR}_{n,j}$ not to be lower than the application required data rate of each SD pair $C^{SD}_{n\_req,j}$, according to Eq. (4). Here, $C^{SD}_{n\_req,j}$ is the required data rate by the IoT application of the nth SD pair; $C^{SD}_{n\_req,j}$ can be different in different time slots for different SD pairs; $C^{SD}_{n\_req,j}$ is assumed fixed and known by the relay BS for each time slot. The rationale of this objective is to maximize the overall data rate for all the source devices and at the same time reduce their energy consumption. From the perspective of a device, transmitting the same amount of data at a higher data rate incurs less transmission time. Less time multiplied by the fixed transmission power indicates less energy consumption in the device. The objective for the first sub-time slot is to

$$\max_{\{W^S_{n,j}\}} \sum_{j=1}^{J} \sum_{n=1}^{N} C^{SR}_{n,j} \quad (6)$$

$$s.t. \ \ C^{SD}_{n\_req,j} \le \frac{1}{2} C^{SR}_{n,j} \quad (7)$$

$$\sum_{j=1}^{J} \sum_{n=1}^{N} W^S_{n,j} \le W_{Relay} \quad (8)$$

$$0 < W^S_{n,j}. \quad (9)$$

Here, Eq. (7) constrains half of the data rate at the SR link not to be less than the data rate required by the nth SD pair. Eq. (8) implies that the total allocated bandwidth for the source devices should be less than or equal to the available bandwidth for the relay D2D group W_{Relay} in this macrocell. $W^S_{n,j}$ is the variable, which is the bandwidth to be allocated to the nth source device in the jth picocell. From Eq. (2), it can be seen that $C^{SR}_{n,j}$ is a concave increasing function of $W^S_{n,j}$. The summation of concave functions, Eq. (6), is still concave [25]. Hence, this optimization problem can be solved efficiently. Each $W^S_{n,j}$ will lead to a corresponding data rate $C^{SR}_{n,j}$ for each SR link. Therefore, the data rates of the SR links are known and fixed for the resource allocation optimization for the subsequent second sub-time slot.

2) Second Sub-time Slot Resource Allocation Optimization: In the first sub-time slot, we have obtained the optimal data rate $C^{SR}_{n,j}$ for each source device, which has been guaranteed to be $\frac{1}{2}C^{SR}_{n,j} \ge C^{SD}_{n\_req,j}$ already. According to Eq. (4), the minimal of $C^{SR}_{n,j}$ and $C^{RD}_{n,j}$ determines the effective data rate between the source and destination device, because one of them will be the bottleneck. Thus, in the second sub-time slot resource allocation optimization, we should guarantee $C^{RD}_{n,j} \geq C^{SR}_{n,j}$ to achieve the IoT application required data rate. By leveraging the relay BS transmission power, the relay BS can enable the RD link to achieve a higher data rate than that of the SR link because the relay BS has much higher transmission power than the mobile device. Therefore, the optimization objective in the second sub-time slot is to minimize all the picocell relay BSs' transmission power for serving all the destination devices in the relay D2D groups in this macrocell, while guaranteeing $C^{RD}_{n,j} \geq C^{SR}_{n,j}$. It is desired to minimize all the relay BSs' energy consumption, no matter whether the relay BSs are powered by green energy or on-grid energy. The objective for the second sub-time slot resource allocation optimization is to

$$\min_{\{P^R_{n,j}, W^R_{n,j}\}} \sum_{j=1}^{J} \sum_{n=1}^{N} P^R_{n,j} \quad (10)$$

$$s.t. \quad C^{SR}_{n,j} \leq C^{RD}_{n,j} \quad (11)$$

$$\sum_{j=1}^{J} \sum_{n=1}^{N} W^R_{n,j} \leq W_{Relay} \quad (12)$$

$$\sum_{n=1}^{N} P^R_{n,j} \leq P_{Total,j} \quad (13)$$

$$0 < W^R_{n,j} \quad (14)$$

$$0 < P^R_{n,j}. \quad (15)$$

Here, Eq. (11) guarantees the data rate of the RD link not to be less than the data rate of the SR link. $W^R_{n,j}$ is the bandwidth for serving the nth destination device in the jth picocell. Eq. (12) implies the total allocated bandwidth for serving the destination devices not to exceed the available W_{Relay} in this macrocell. $P^R_{n,j}$ is the relay BS transmission power for serving the nth destination device. Owing to the hardware limitation, $P_{Total,j}$ is the maximum transmission power of the relay BS j; Eq. (13) imposes the total transmission power for serving the destination devices not to exceed its maximum transmission power $P_{Total,j}$. It can be proved that this optimization problem is a convex problem, and hence its optimal solution can be obtained efficiently.

Proposition 1. *The second sub-time slot resource allocation optimization problem is a convex problem.*

Proof: According to Eq. (3), the transmission power at the jth relay BS for serving the nth destination device $P^R_{n,j}$ can be expressed as

$$P^R_{n,j} = (2^{\frac{C^{RD}_{n,j}}{W^R_{n,j}}} - 1) \cdot \frac{N_0 W^R_{n,j}}{h^{RD}_{n,j}}. \quad (16)$$

Hence, the objective function Eq. (10) and its constraints can be re-written as

$$\min_{\{W^R_{n,j}, C^{RD}_{n,j}\}} \sum_{j=1}^{J} \sum_{n=1}^{N} (2^{\frac{C^{RD}_{n,j}}{W^R_{n,j}}} - 1) \cdot \frac{N_0 W^R_{n,j}}{h^{RD}_{n,j}} \quad (17)$$

$$s.t. \quad C^{SR}_{n,j} \leq C^{RD}_{n,j} \quad (18)$$

$$\sum_{j=1}^{J} \sum_{n=1}^{N} W^R_{n,j} \leq W_{Relay} \quad (19)$$

$$\sum_{n=1}^{N} P^R_{n,j} \leq P_{Total,j} \quad (20)$$

$$0 < W^R_{n,j} \quad (21)$$

$$0 < C^{RD}_{n,j}. \quad (22)$$

Here, $W^R_{n,j}$ and $C^{RD}_{n,j}$ are the only variables in Eq. (17); the values of other notations are all given. By calculating the second-order derivatives, the Hessian matrix of Eq. (16) is positive semidefinite. That is, Eq. (16) is a convex function [25]. The summation of convex functions, Eq. (17), is still convex [25]. The inequality constraints (18)-(20) are also convex. Hence, this optimization problem is convex. ■

C. Green Energy Balancing Optimization with Dual Batteries

By installing dual batteries at relay BSs, the amount of available green energy for each time period is known and accurate. This time period is called battery cycle in this paper. The mechanism is simple, in which the relay BS consumes the green energy stored in Battery 1 in the current battery cycle that was harvested in the previous battery cycle. Then, in the next battery cycle, the relay BS consumes the green energy stored in Battery 2 that is harvested in the current battery cycle. That is, the two batteries alternate their roles of harvesting and discharging in every battery cycle at a relay BS. Since rechargeable energy storage devices cannot both charge and discharge simultaneously [26], this is the reason dual batteries are required. We consider solar energy harvested from solar panels at the relay BSs as the green energy source in this work though other renewal sources can be equally adopted.

We denote T as the battery cycle and T is selected to be an integer multiple of time slot τ. At the beginning of each battery cycle, the initial total available green energy in a battery of relay BS j is E^0_j, which was harvested in the previous battery cycle. E^0_j can be different in different battery cycles at the same or a different relay BS j, and has to be less than or equal to the full battery capacity. As time elapses during the battery cycle, the residual green energy in the battery of relay BS j at the tth time slot is E^t_j. $0 \leqslant E^t_j \leqslant E^0_j$ constrains E^t_j to be between zero and the initial green energy E^0_j stored in the battery. E^t_j at the relay BS j is updated for each time slot t. In Eq (10), we have obtained the energy consumption $\sum_{n=1}^{N} P^R_{n,j}$ for each relay BS of each time slot. Since this amount of energy is only consumed in every second sub-time slot, the energy consumption of relay BS j during the tth time slot can be expressed as

$$K^t_j = \sum_{n=1}^{N} P^R_{n,j} \frac{\tau}{2} + P^{static}_j \tau, \quad (23)$$

and P^{static}_j is the static power consumption of BS j.

Based on our proposed architecture, the relay BSs are connected with each other not only by networking cables/fibers, but also connected by electric transmission lines for balancing residual green energy[2]. Transferring green energy among local relay BSs is more efficient than delivering on-grid energy from a remote power plant, in terms of electricity transmission loss [27]. In every time slot, according to the energy consumption K_j^t of the relay BSs and the residual green energy E_j^t in their batteries, the green energy balancing execution policy adopts the guideline below. Guideline 1 is motivated by the following intuition. When some relay BSs do not have sufficient green energy to accommodate their communication workloads, the other relay BSs with abundant green energy may transmit electricity to supplement those relay BSs with insufficient green energy. Thus, those relay BSs can first temporally utilize green energy, instead of consuming on-grid energy immediately. This guideline maximizes the utilization of the available green energy in a macrocell and furthest reduces on-grid energy consumption.

Guideline 1.

1) When all the relay BSs have sufficient residual green energy to supplement their workloads demanded energy in each time slot, i.e., $E_j^t \geq K_j^t$, the relay BSs directly drain the energy from their own batteries.
2) Once one relay BS has insufficient residual green energy to accommodate its communication workload in the current time slot, i.e., $E_j^t < K_j^t$, then this relay BS is classified into a set, $\boldsymbol{S_1}$. The rest of relay BSs with sufficient residual green energy are classified into the other set, $\boldsymbol{S_2}$, and each relay BS in this set is indexed by i. According to the amount of their residual green energy, the relay BSs in $\boldsymbol{S_2}$ will transmit their electricity to the relay BS in $\boldsymbol{S_1}$, to supplement the shortage of green energy.
3) As more relay BSs exhaust their green energy, the number of relay BSs in $\boldsymbol{S_1}$ increases. Relay BSs in $\boldsymbol{S_2}$ continuously transmit electricity to relay BSs in $\boldsymbol{S_1}$. When the total green energy shortage in $\boldsymbol{S_1}$, $\sum_{j \in \boldsymbol{S_1}} (K_j^t - E_j^t)$, is larger than the total surplus green energy in $\boldsymbol{S_2}$, $\sum_{i \in \boldsymbol{S_2}} (E_i^t - K_i^t)$, the relay BSs in $\boldsymbol{S_2}$ only transmit green energy to those in a subset of $\boldsymbol{S_1}$, i.e., $\boldsymbol{S_1'} \subset \boldsymbol{S_1}$, with $\sum_{j \in \boldsymbol{S_1'}} (K_j^t - E_j^t) < \sum_{i \in \boldsymbol{S_2}} (E_i^t - K_i^t)$.
4) When all the relay BSs belong to $\boldsymbol{S_1}$, the relay BSs stop transmitting electricity between each other.

In practice, the electric power transmission efficiencies of the electric transmission lines between each pair of relay BSs are different. Transmitting electricity through the electric transmission lines leads to some electricity loss. Here, our goal is to minimize the electricity loss when the electricity is transmitted among the relay BSs, i.e., maximizing the amount of effective electricity transmitted along the transmission lines. We will determine which relay BSs in $\boldsymbol{S_2}$ should transmit to which relay BSs in $\boldsymbol{S_1}$ or $\boldsymbol{S_1'}$ by how much electricity for the above Steps 2) and 3). Assume every two relay BSs in a macrocell are connected by an electric transmission line. We use i, j to denote two different relay BSs in a macrocell, respectively. Here, $i \in \boldsymbol{S_2}$ and $j \in \boldsymbol{S_1}$ or $\boldsymbol{S_1'}$. $\theta_{i,j}$ is the electric transmission line loss-rate between relay BS i and j. $0 < \theta_{i,j} < 1$ is assumed known in advance, according to the distance between the relay BSs and the material of the electric transmission line. A higher $\theta_{i,j}$ implies a larger electricity transmission loss, i.e., lower electricity transmission efficiency. $\delta_{i,j}$ represents the amount of electricity (green energy) to be transmitted from relay BS i to relay BS j. The objective is to minimize the amount of electricity transmission loss in this macrocell, and so the objective is to

$$\min_{\{\delta_{i,j}\}} \sum_{i \in \boldsymbol{S_2}, j \in \boldsymbol{S_1}/\boldsymbol{S_1'}} \theta_{i,j}\delta_{i,j} \tag{24}$$

$$s.t. \sum_{i \in \boldsymbol{S_2}, j \in \boldsymbol{S_1}} (1-\theta_{i,j})\delta_{i,j} = \sum_{j \in \boldsymbol{S_1}/\boldsymbol{S_1'}} (K_j^t - E_j^t) \tag{25}$$

$$0 \leq \delta_{i,j} \leq E_i^t - K_i^t \tag{26}$$

$$0 < \theta_{i,j} < 1. \tag{27}$$

The left side term of Eq. (25) is the effective amount of electricity transmitted from the relay BSs in $\boldsymbol{S_2}$ to those in $\boldsymbol{S_1}$ or $\boldsymbol{S_1'}$ in this macrocell, and the right side term of Eq. (25) is the amount of energy requested from the relay BSs in $\boldsymbol{S_1}$ or $\boldsymbol{S_1'}$ to supplement their green energy shortage. The left side term equaling to the right side term means all the requested energy from $\boldsymbol{S_1}$ or $\boldsymbol{S_1'}$ is fulfilled by the relay BSs in $\boldsymbol{S_2}$. Eq. (26) constrains $\delta_{i,j}$ to be between zero and the amount of surplus green energy of relay BS i at current time slot t. Since this green energy balancing problem is a linear programming problem and $\delta_{i,j}$ is the only variable, it can be solved efficiently. This green energy balancing optimization policy guarantees all the green energy harvested in this network to be fully utilized first, thus achieving the goal of furthest reducing the on-grid energy consumption.

IV. Simulations

Simulations are set up as follows. One macrocell contains 6 picocells. The radius of this macrocell is $750m$. The picocell relay BSs are deployed uniformly within this macrocell, and their locations are fixed. The distribution of devices is generated by the Poisson point process (PPP) in this macrocell [28]. The distance-dependent channel model [17] is adopted in simulations. Within each time slot $\tau = 10ms$, the devices' locations are fixed. Each device is arbitrarily assigned one level of transmission power, either $200mW$ or $300mW$; within each time slot, the transmission power of a source device is fixed. Within the coverage of each picocell, the pairing for the SD pairs is arbitrarily assigned. Also, the IoT application required data rate of each SD pair is arbitrarily assigned among 2Mbps, 6Mbps and 10Mbps; within each time slot, the required data rate is fixed. The total available bandwidth in a macrocell for D2D communications is 20MHz. The electric transmission line loss-rate $\theta_{i,j}$ between every two relay BSs are randomly generated between 5% and 10%, and fixed in the experiments.

Fig. 4 shows the average available bandwidth for the relay D2D group versus the number of SD pairs in the direct D2D group in a macrocell. This figure presents the Monte Carlo

[2]The optimal deployment of networking cables/fibers and electric transmission lines is out of the scope of this paper.

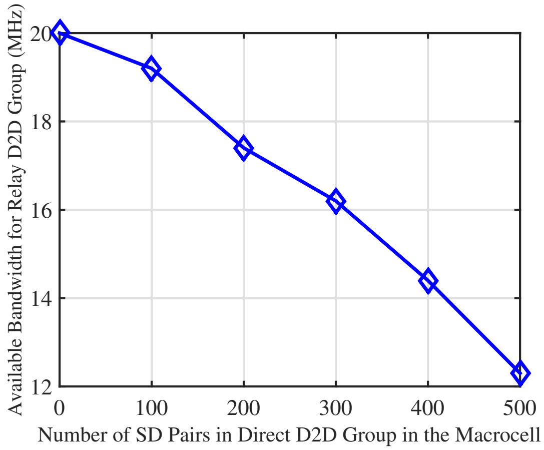

Fig. 4. The average available bandwidth for relay D2D group.

result obtained from one thousand repeated experiments. In these experiments, we fix the total number of SD pairs as 1000 and record the number of SD pairs in the direct D2D group of this macrocell and the corresponding average available bandwidth for the relay D2D group. The decreasing line implies that the more SD pairs belong to the direct D2D group, the less available bandwidth for the relay D2D group because by executing our resource allocation method, we allocate the spectrum to the direct SD pairs first. In each experiment, as the number of SD pairs in the direct D2D group increases, the required bandwidth increases. As the total bandwidth for IoT D2D communications is fixed, the more bandwidth used by the direct D2D group, the less available bandwidth left for the relay D2D group. In theory, if all the SD pairs belong to the direct D2D group (owing to the proximity of SD devices with very good channel condition), then there will be no SD pairs in the relay D2D group and we can allocate all the spectrum for the direct D2D transmissions. If this is the case, our architecture achieves the pure and ideal D2D communications, i.e., all the SD pairs can directly communicate, and no energy is consumed at the relay BSs for relaying data.

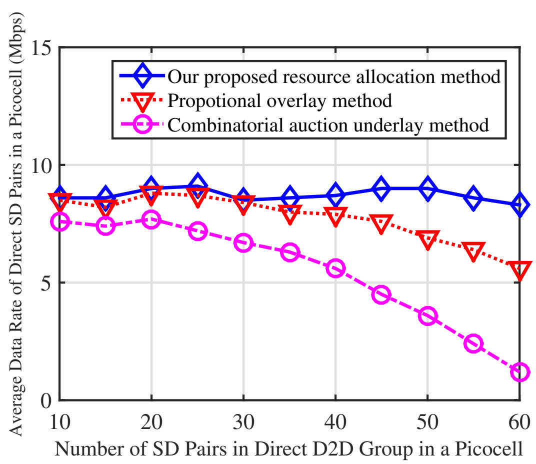

Fig. 5. The average data rate of SD pairs in the direct D2D group.

Fig. 5 shows the average data rate of the direct SD pairs in a picocell with different numbers of SD pairs in the direct D2D group. We randomly choose a picocell in the macrocell to observe the performance of different resource allocation methods on the average data rate with different numbers of direct SD pairs. The top blue curve with diamond marks nearly remains unchanged with the increasing number of SD pairs in the direct D2D group because our proposed resource allocation method allocates the spectrum to the direct D2D group first to fulfill their IoT applications required bandwidth. We serve the direct SD pair as the "preferred user", and the remaining spectrum is allocated for the relay D2D group. Since the average required data rate of different types of D2D devices in the network is stable, the blue curve keeps nearly unchanged. The red curve with triangle marks represents the performance of a comparison method [28], which partitions the cellular spectrum into two parts, one part for cellular usage and the other part for D2D usage. The red curve performs almost the same as our proposed method with a small number of D2D pairs, but it deteriorates when more SD pairs transmit because in their proportional overlay spectrum sharing method, D2D users share channels to transmit; when more D2D users start their transmissions, their data rates are affected by the co-channel interference. Thus, the decreasing rate of the red curve is determined by the spectrum partition factor in [28]. The purple curve with circular marks is the performance of another comparison method [17], which degrades rapidly because in their iterative combinatorial auction underlay spectrum sharing method, the D2D user has to adjust its transmission power in order to avoid harmful interference to the cellular users, but it receives the interference from other co-channel D2D users as well as cellular users.

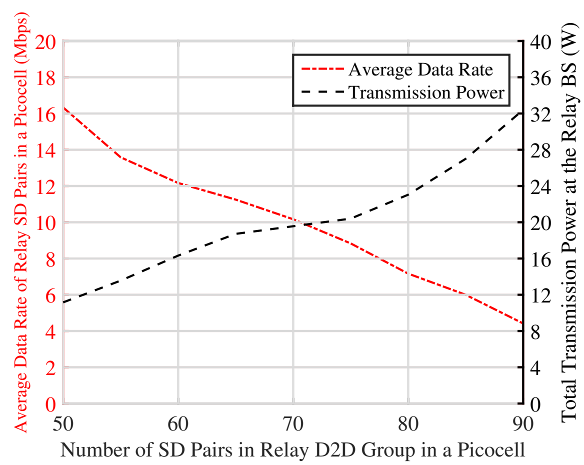

Fig. 6. The average data rate and the relay BS total transmission power.

Fig. 6 shows the average data rate of the relay SD pairs and the relay BS transmission power versus the number of SD pairs in the relay D2D group in a picocell. As the number of relay SD pairs increases, the average data rate of the relay SD pair in this group decreases because when more relay SD pairs share the limited bandwidth left for the relay D2D group, the available bandwidth for facilitating individual transmissions is less. Meanwhile, as the number of SD pairs increases, the total relay BS transmission power for serving the destination devices also increases, because more RD links are served by the relay BS.

In the simulations, the battery cycle is set as T =60 minutes. We define the capacity of each single battery to be 2kWh. The

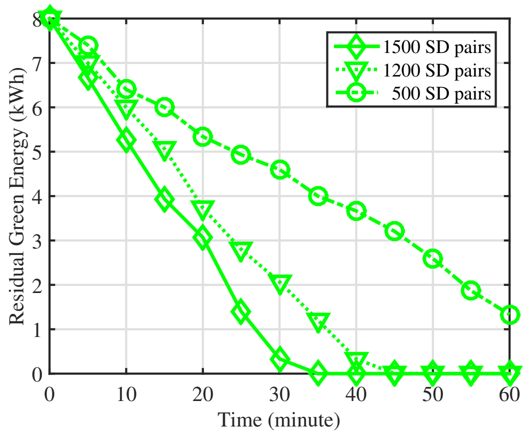

Fig. 7. Residual green energy in the macrocell.

initial available green energy at the beginning of the battery cycle for the 6 relay BSs in a macrocell is arbitrarily assigned between 0.8kWh and 1.6kWh, and we set the amount of total initial available green energy at these 6 relay BSs to be 8kWh. Fig. 7 shows the residual green energy left in a macrocell with different SD pair densities, i.e., 1500 SD pairs, 1200 SD pairs, and 500 SD pairs, respectively. As shown in this figure, when the network has a higher SD pair density, green energy in the network is exhausted quicker. The relay BSs (in $\boldsymbol{S_2}$) with sufficient residual green energy will transmit their electricity via electric transmission lines to the relay BSs (in $\boldsymbol{S_1}$ or $\boldsymbol{S_1'}$) which run out of green energy. By balancing the residual green energy in the network, our proposed architecture maximizes the green energy utilization and achieves the goal of furthest saving the on-grid energy. When the network has a low SD pair density, green energy in the network will not be used up at the end of battery cycle, and thus on-gird energy is not drawn.

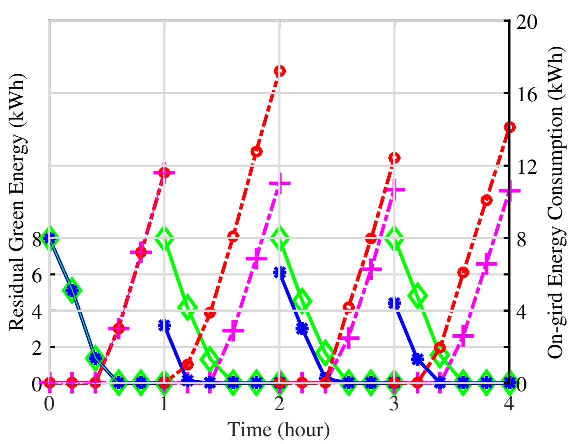

Fig. 8. Performance comparison between the scenarios with single battery and dual batteries.

Fig. 8 shows the performance comparison between the scenarios with single battery and dual batteries for serving 1500 SD pairs. In the single battery scenario, each relay BS is equipped with single battery. When the battery exhausts its green energy, it starts to harvest green energy (recharge); when the next battery cycle begins, all the single batteries in the network start to power the relay BSs. In Fig. 8, the blue curve with star marks and the red curve with circular marks indicate the residual green energy and on-grid energy consumption of the single battery scenario, respectively. The green curve with diamond marks and the purple curve with cross marks present the residual green energy and on-grid energy consumption of the dual batteries scenario, respectively. The two scenarios perform the same in the first battery cycle (Hour 1) because we initialize the same residual green energy for both scenarios and assume they experience the same communications workload. In the beginning of the second battery cycle (Hour 2), the single battery scenario's total harvested green energy is less than that in the dual batteries scenario because in the single battery scenario, in Hour 1, the single battery first spends some time to power the relay BS to exhaust its green energy, then turns into the recharging mode to harvest green energy. Its green energy harvesting (recharging) time is less than a full battery cycle. In comparison, in the dual batteries scenario, the two batteries alternately harvest green energy and power the relay BS, and therefore, when the first battery cycle ends, the second battery is well recharged by harvesting green energy; its harvested green energy is more than that in the single battery scenario. In the single battery scenario, less harvested green energy is exhausted quicker in each battery cycle; less portion of time utilizing green energy implies more on-grid energy to be supplementarily consumed.

V. Conclusion

We have proposed a novel architecture by adopting the overlay spectrum sharing approach and green relay BSs to facilitate D2D communications for IoT in heterogeneous cellular networks. In each macrocell, by optimizing the network resource allocation, the required data rates of the SD pairs of IoT applications have been satisfied and all the relay BSs' overall communication energy consumption is minimized. By equipping dual batteries at each relay BS, unlike most existing green energy related works, we do not need to predict the available green energy. The amount of available green energy at a relay BS in each time period is known and accurate. By balancing the residual green energy among the relay BSs, the utilization of green energy has been maximized and achieves the goal of furtherest saving on-grid energy. We have validated the performance of the proposed novel architecture through extensive simulations.

References

[1] X. Liu and N. Ansari, "Green relay assisted D2D communications with dual battery for IoT," *IEEE Globecom 2016*, pp. 1–6, Dec. 2016.

[2] ETSI, "Low throughput networks (LTN): Use case, functional architecture, and protocols," *ETSI GS LTN 001*, Sept. 2014.

[3] M. R. Palattella *et al.*, "Internet of things in the 5G era: Enablers, architecture, and business models," *IEEE JSAC*, vol. 34, no. 3, pp. 510–527, 2016.

[4] M. N. Tehrani, M. Uysal, and H. Yanikomeroglu, "Device-to-device communication in 5G cellular networks: challenges, solutions, and future directions," *IEEE Commun. Mag.*, vol. 52, no. 5, pp. 86–92, 2014.

[5] X. Lin *et al.*, "An overview of 3GPP device-to-device proximity services," *IEEE Commun. Mag.*, vol. 52, no. 4, pp. 40–48, 2014.

[6] J. Liu, N. Kato, J. Ma, and N. Kadowaki, "Device-to-device communication in LTE-advanced networks: a survey," *IEEE Commun. Suv. & Tut.*, vol. 17, no. 4, pp. 1923–1940, 2014.

[7] C.-H. Yu *et al.*, “Resource sharing optimization for device-to-device communication underlaying cellular networks,” *IEEE Trans. on Wireless Commu.*, vol. 10, no. 8, pp. 2752–2763, 2011.
[8] J. G. Andrews *et al.*, “What will 5G be?” *IEEE JSAC*, vol. 32, no. 6, pp. 1065–1082, 2014.
[9] GSM-Association, “5G Spectrum.” [Online]. Available: http://www.gsma.com/spectrum/wp-content/uploads/2015/04/5G-Spectrum-Policy-Position-FINAL.pdf
[10] FCC, “Fact sheet: spectrum frontiers rules identify, open up vast amount of new high-band spectrum for next generation (5G) wilress broadband.” [Online]. Available: http://apps.fcc.gov/edocs_public/attachmatch/DOC-340310A1.pdf
[11] Y. Wu *et al.*, “Device-to-device meets LTE-unlicensed,” *IEEE Commun. Mag.*, vol. 54, no. 5, pp. 154–159, 2016.
[12] B. Ren *et al.*, “Cellular communications on license-exempt spectrum,” *IEEE Communications Magazine*, vol. 54, no. 5, pp. 146–153, 2016.
[13] X. Liu, T. Han, and N. Ansari, “Intelligent battery management for cellular networks with hybrid energy supplies,” *IEEE WCNC, 2016*, pp. 1–6, Apr. 2016.
[14] T. Han and N. Ansari, “On optimizing green energy utilization for cellular networks with hybrid energy supplies,” *IEEE Trans. on Wireless Commun.*, vol. 12, no. 8, pp. 3872–3882, Aug. 2013.
[15] Ansari, Nirwan and Han, Tao, *Green Mobile Networks: A Networking Perspective*. Wiley-IEEE Press, 2017.
[16] X. Liu, X. Huang, and N. Ansari, “Green energy driven user association in cellular networks with dual battery system,” *IEEE ICC 2016*, pp. 1–6, May. 2016.
[17] F. Wang *et al.*, “Energy-efficient resource allocation for device-to-device underlay communication,” *IEEE Trans. on Wireless Commun.*, vol. 14, no. 4, pp. 2082–2092, 2015.
[18] T. Han and N. Ansari, “ICE: Intelligent cell breathing to optimize the utilization of green energy,” *IEEE Commun. Letters*, vol. 16, no. 6, pp. 866–869, Jun. 2012.
[19] B. Wang *et al.*, “Resource allocation optimization for device-to-device communication underlaying cellular networks,” *Pro. VTC*, vol. IEEE 73rd, pp. 1–6, 2011.
[20] D. Lopez-Perez *et al.*, “Enhanced intercell interference coordination challenges in heterogeneous networks,” *IEEE Wireless Commun.*, vol. 18, no. 3, pp. 22–30, 2011.
[21] J. Liu *et al.*, “Device-to-device communications achieve efficient load balancing in LTE - advanced networks,” *IEEE Wireless Commun.*, vol. 21, no. 2, pp. 57–65, 2014.
[22] G. Zhao *et al.*, “Power and channel allocation for cooperative relay in cognitive radio networks,” *J. Sel. Top. Sig. Proc.*, vol. 5, no. 1, pp. 151–159, 2011.
[23] T. Han and N. Ansari, “Heuristic relay assignments for green relay assisted device to device communications,” *IEEE GLOBECOM 2013*, vol. 20, pp. 468–473, 2013.
[24] Shannon, Claude E and Weaver, Warren, *The mathematical theory of communication*. University of Illinois press, 2002.
[25] Boyd, Stephen and Vandenberghe, Lieven, *Convex optimization*. Cambridge university press, 2004.
[26] S. Luo, R. Zhang, and T. Lim, “Optimal save-then-transmit protocol for energy harvesting wireless transmitters,” *IEEE Trans. Wireless Commun.*, vol. 12, no. 3, pp. 1196–1207, Mar. 2013.
[27] N. B. Negra, J. Todorovic, and T. Ackermann, “Loss evaluation of HVAC and HVDC transmission solutions for large offshore wind farms,” *Electric Power Systems Research*, vol. 76, no. 11, pp. 916–927, 2006.
[28] X. Lin, J. G. Andrews, and A. Ghosh, “Spectrum sharing for device-to-device communication in cellular networks,” *IEEE Trans. on Wireless Commun.*, vol. 13, no. 12, pp. 6727–6740, 2014.

Xilong Liu (S’14) received the B.E. degree in Telecommunication Engineering from the Zhengzhou University, Zhengzhou, China, in 2011, the M.S. degree in Electrical Engineering from the New Jersey Institute of Technology (NJIT), Newark, NJ, USA and is currently working toward the Ph.D. degree in Electrical Engineering at NJIT. His research interests include mobile and wireless networking, green communications, network optimization, device-to-device communications, and Internet of Things.

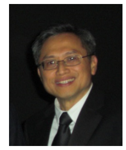

Nirwan Ansari (S’78-M’83-SM’94-F’09) is Distinguished Professor of Electrical and Computer Engineering at the New Jersey Institute of Technology (NJIT). He has also been a visiting (chair) professor at several universities.

Professor Ansari has authored *Green Mobile Networks: A Networking Perspective* (IEEE-Wiley, 2017) with T. Han, and co-authored two other books. He has also (co-)authored more than 500 technical publications, over 200 published in widely cited journals/magazines. He has guest-edited a number of special issues covering various emerging topics in communications and networking. He has served on the editorial/advisory board of over ten journals. His current research focuses on green communications and networking, cloud computing, and various aspects of broadband networks.

Professor Ansari was elected to serve in the IEEE Communications Society (ComSoc) Board of Governors as a member-at-large, has chaired ComSoc technical committees, and has been actively organizing numerous IEEE International Conferences/Symposia/Workshops. He has frequently been delivering keynote addresses, distinguished lectures, tutorials, and invited talks. Some of his recognitions include several Excellence in Teaching Awards, a few best paper awards, the IEEE GCCTC Distinguished Technical Achievement Recognition Award, the ComSoc AHSN TC Technical Recognition Award, Purdue University Outstanding Electrical and Computer Engineer Award, the NCE Excellence in Research Award, the NJ Inventors Hall of Fame Inventor of the Year Award, the Thomas Alva Edison Patent Award, and designation as a COMSOC Distinguished Lecturer. He has also been granted over 30 U.S. patents.

He received a Ph.D. from Purdue University in 1988, an MSEE from the University of Michigan in 1983, and a BSEE (summa cum laude with a perfect GPA) from NJIT in 1982.